International Journal of Control and Automation
Vol.6, No.5 (2013), pp.21-30
http://dx.doi.org/10.14257/ijca.2013.6.5.03

Measuring and Comparison of Edge Detectors in Color Spaces

Gwanggil Jeon

Department of Embedded Systems Engineering, Incheon National University
12-1 Songdo-dong, Yeonsu-gu, Incheon 406-772, Korea

gjeon@incheon.ac.kr

Abstract

Edge detection has been a popular practice in image processing and computer vision applications. Many image processing applications require the discovery of edge details in the gray or color images as a beginning stage of an image processing, vision and understanding. Generally, edge detection on grayscale images is not affluent enough to explain intensity changes. Therefore, we can use color edge information as an important method. Because the result is different when input images are color images or not (grayscale images). The main purpose of the proposed edge detection is to discern significant parts from the normal features in a given image. We assume that intensity varies rapidly in a significant part. There are many color spaces such as RGB, YIQ, and HSV (Hue, Saturation, and Value). In this paper, we conducted edge detection on each color spaces and compared the results. Simulation results show that the HSV color space gives the best detection performance.

Keywords: *edge detection, HSV color space, image understanding, color conversion*

1. Introduction

The edges are known as surprising intensity variation in the gray or color levels in an image. The edge detection is to detect edges in an image which is a significant tool which makes a binary image from the original one by extracting informative object boundaries. Thus, the edge detection is a crucial topic in image processing, understanding and computer vision. After the edge detection, the information of an image to be operated is intensely reduced because the image contains only object boundaries. The edge detection classifies an image into object and background. The performance of edge detection is favorably contingent upon noise, presence of similar intensity objects, lighting, and density of edges in the scene [1-3].

The grayscale of a pixel is normally provided as one intensity value, while the color of a pixel is given as three intensity values pointing out the tri-stimuli of red (R), green (G) and blue (B). It is known that edge detection on grayscale images is not fully enough to describe intensity changes. Therefore, color edge information can be considered to support the shortage of result of grayscale images. There have been many approached in literature [4-6]. It is known that various edge detectors operate better under certain conditions. Therefore, applying multiple edge detectors in a multi color channels give better results. We tested Sobel edge detector on different color channels.

In this paper, we use Sobel mask on different color spaces and compare the results with other results from color spaces. Again, the edge detection is an important tool in image processing [7-23]. We used three color spaces: RGB, YIQ and HSV, where RGB stands for red, green and blue, YIQ means color space designed for the NTSC color TV system, and HSV is hue, saturation, and value, respectively. The Sobel mask is used in sub-channel of

ISSN: 2005-4297 IJCA

each color spaces, and eventually the most appropriate color space for edge detection is used. This paper is organized as follows. Section 2 explains the color space comparison between RGB, YIQ, and HSV. The Sobel mask is described in Section 3, and the simulation results and its subjective performance comparison are depicted in Section 4. The conclusions are made in Section 5.

2. Color Channels for Edge Detection

In general, a color is denoted by RGB intensities. The RGB color space is converted into YIQ or HSV color spaces. It is known that the hue component or HSV color space is indicated as the fraction around the ring beginning from red color, [1 0 0]. Similarly, each color channel has different hue value. Table 1 shows color-hue comparison.

Table 1. Color-hue comparison

Color	Red	Yellow	Green	Cyan	Blue	Magenta
Hue	0	0.1667	0.3333	0.5	0.6667	0.8333

We are given three R, G, B intensity values. These values are ranging from 0 to 1 or 0 to 255. If these values are bigger than 1, then we can divide them by 255. Then, we obtain $\max_{RGB}$, Δ, and S as follows:

$$\begin{aligned} \max_{RGB} &= \max\{R,G,B\} \\ \Delta &= \max_{RGB} - \min\{R,G,B\} \\ S &= \frac{\Delta}{\max_{RGB}} \end{aligned} \quad (1)$$

Then, the hue values can be found as

$$\begin{aligned} &\text{If } R = \max_{RGB}, \text{ then } H = \frac{1}{6}\left(\frac{G-B}{\Delta}\right) \\ &\text{Else if } G = \max_{RGB}, \text{ then } H = \frac{1}{6}\left(2+\frac{B-R}{\Delta}\right) \\ &\text{Else if } B = \max_{RGB}, \text{ then } H = \frac{1}{6}\left(4+\frac{R-G}{\Delta}\right) \end{aligned} \quad (2)$$

Here is an example. If (R,G,B) is (0.4,0.6,0.8), then we have

$$\begin{aligned} \max_{RGB} &= \max\{0.4, 0.6, 0.8\} = 0.8 \\ \Delta &= \max_{RGB} - \min\{R,G,B\} = 0.8 - 0.4 = 0.4 \\ S &= \frac{\Delta}{\max_{RGB}} = \frac{0.4}{0.8} = 0.5 \end{aligned} \quad (3)$$

Here, we found $\max_{RGB} = B$, therefore H is obtained as

$$H = \frac{1}{6}\left(4+\frac{0.4-0.6}{0.4}\right) = 0.5833 \quad (4)$$

The converting process from HSV to RGB is opposite process.

As mentioned before, the YIQ color space is used for TV and video in America, Canada, Japan and Korea. These countries normally use NTSC (National Television System Committee). The YIQ uses one luminance channel, Y, and three color channels I and Q. The Y contains intensity or luminance, and I and Q contain color information. The conversion equation is quite simple to implement. **M** is the matrix conversion kernel.

$$\mathbf{M} = \begin{bmatrix} 0.299 & 0.587 & 0.114 \\ 0.596 & -0.274 & -0.321 \\ 0.211 & -0.523 & 0.311 \end{bmatrix} \tag{5}$$

Then, the forward conversion (RGB to YIQ) and the inverse conversion are conducted as Eqs. (6) and (7).

$$\begin{bmatrix} Y \\ I \\ Q \end{bmatrix} = \mathbf{M} \begin{bmatrix} R \\ G \\ B \end{bmatrix}. \tag{6}$$

$$\begin{bmatrix} R \\ G \\ B \end{bmatrix} = \mathbf{M}^{-1} \begin{bmatrix} Y \\ I \\ Q \end{bmatrix}. \tag{7}$$

3. Existing Edge Detection Algorithm

Edges contain some important information in an image. We can use edges to measure the size of object in an image. There are large number of edge detection and finding algorithms. The aim of this study is to aid the selection of appropriate operator that is able to detect edge boundaries based on intensity discontinuities. For example, Prewitt filter uses

$$P_x = \begin{bmatrix} -1 & 0 & -1 \\ -1 & 0 & -1 \\ -1 & 0 & -1 \end{bmatrix} \text{ and } P_y = P_x^T. \tag{8}$$

And the gradient f at coordinates (x,y) is defined as

$$|\nabla f(x,y)| = \sqrt{(\partial_x f(x,y))^2 + (\partial_y f(x,y))^2}\ . \tag{9}$$

The Prewitt filter extracts edges utilizing the Prewitt estimate to the derivative. It replies edges at those pixels where the image gradient is the biggest. The results of implementing Prewitt filter is shown in Figure 1(c).

The Roberts cross-gradient filter uses approximation shown in Eq. (10).

$$R_1 = \begin{bmatrix} 1 & 0 & 0 \\ 0 & -1 & \\ 0 & 0 & 0 \end{bmatrix} \text{ and } R_2 = \begin{bmatrix} 0 & 1 & 0 \\ -1 & 0 & \\ 0 & 0 & 0 \end{bmatrix}. \tag{10}$$

Roberts filter extracts pixels utilizing Roberts estimate to the derivative. It replies edges at those pixels where the gradient of the image is the biggest. The results of implementing Roberts filter is shown in Figure 1(d). Finally, the Sobel filters use

$$S_x = \begin{bmatrix} -1 & 0 & -1 \\ -2 & 0 & -2 \\ -1 & 0 & -1 \end{bmatrix} \text{ and } S_y = S_x^{\ T}. \tag{11}$$

The Sobel filter extracts pixels using the Sobel estimate to the derivative. It replies edges at those pixels where the gradient of the image is the biggest. The results of implementing Roberts filter is shown in Figure 1(e).

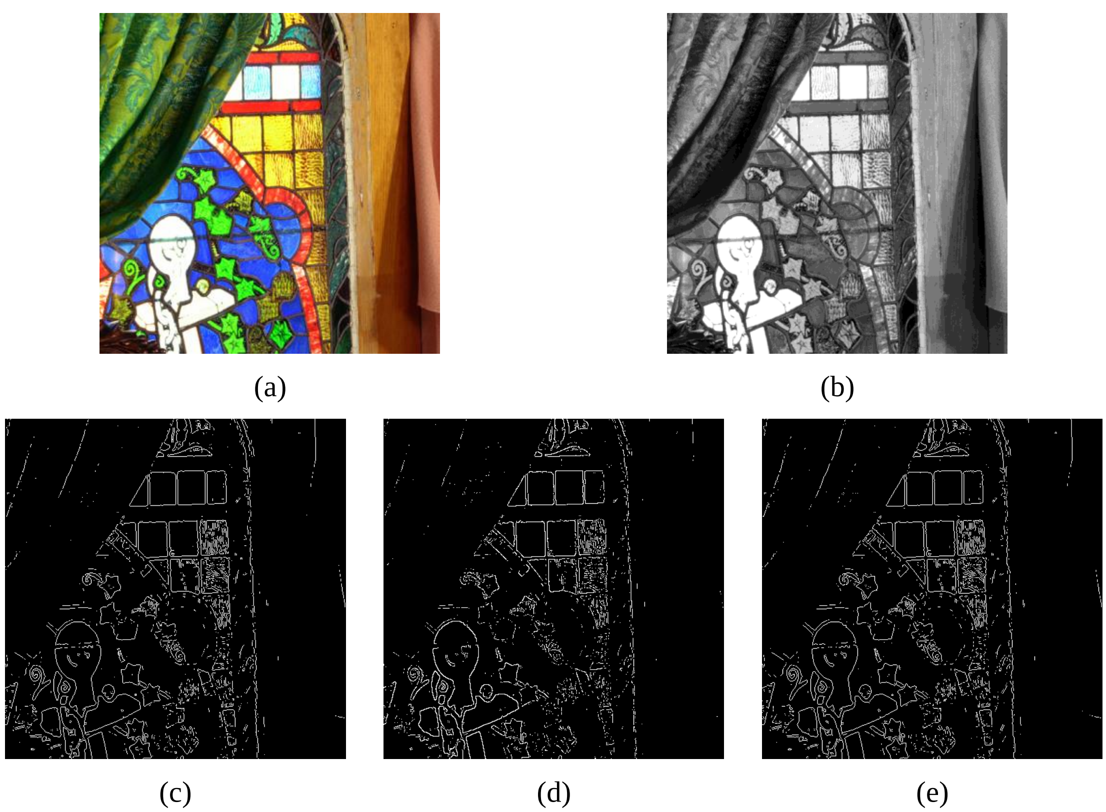

Figure 1. Example of detected edges: (a) McM image #1, (b) grayscale image of (a), (c) Prewitt filters, (d) Roberts filters, and (e) Sobel filters

4. Simulation Results

To evaluate the accuracy of the described three edge detection methods, some simulations have been carried out on four LC images #46-#49 as shown in Figure 1. These images can be downloaded [24]. The original images have been cropped by 256×256 images. The test images are shown in Figure 2, and the result images are shown in Figures 3-4. For RGB color space case, images in Figure 4 shows the detected edges which come from red (*R* channel), green (*G* channel), and blue (*B* channel). For YIQ color space case, red, green, and blue edges come from *Y*, *I*, and *Q* channels, respectively. For HSV color space case, red, green, and blue edges come from *H*, *S*, and *V* channels, respectively. To obtain grayscale image, all color images were converted to grayscale using a function of Matlab (*rgb2gray*).

Figure 2. Test LC images #46-#49 images

The first feature that we can notice on result images is that all three methods give satisfactory results. However, edges from Prewitt and Roberts are often disconnected and spotty. Sometimes it was hard to trace disconnected points in a line, which is not recommended for suitable method.

In order to test better color image edge detection, we analyzed the existing edge detectors with three color spaces, RGB, YIQ, and HSV. To obtain edges from HSV color space, color image characteristics is considered, and the space is separated by hue, saturation and value information. After the Sobel mask applied we could obtain Figures 3 and 4. As we can see, Sobel mask on HSV color space gives the pleasant and distinct edges. Also, HSV color space provides more real edges with better continuity.

(a) (b) (c)

Figure 3. Obtained edges by different edge detection methods on LC #46-#49 images: (a) RGB color space, (b) YIQ color space, and (c) HSV color space

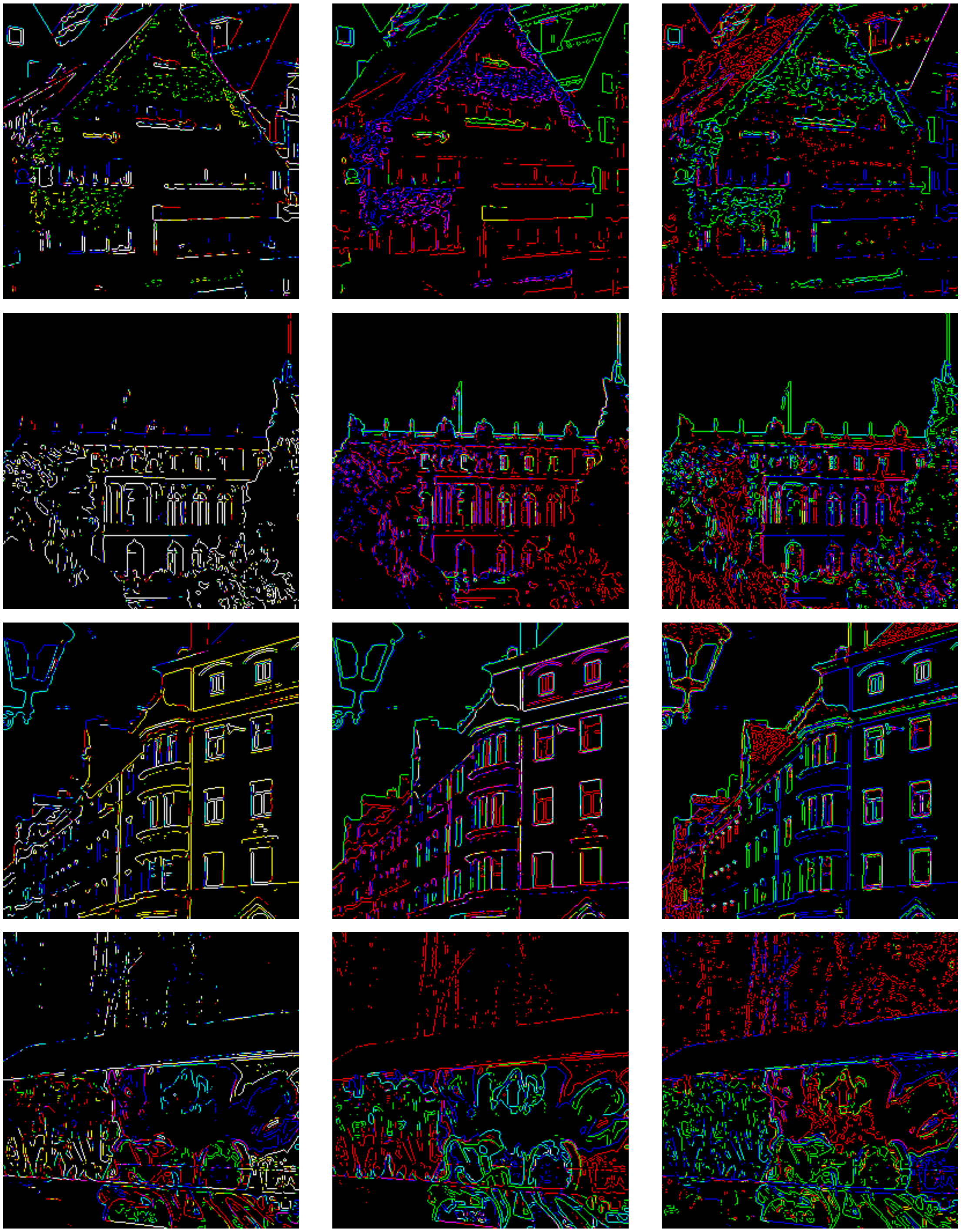

(a) (b) (c)

Figure 4. Obtained edges by different edge detection methods on LC #46-#49 images: (a) RGB color space, (b) YIQ color space, and (c) HSV color space

5. Conclusions

Edge detection algorithm is one of main image processing tools. In this paper, we considered three well known color spaces: RGB, YIQ, and HSV. We applied Sobel method on above three color spaces and evaluated the performance From the experimental results section, it was noticed that the results from HSV color space is better than the others.

Acknowledgements

This work was supported in part by the National Science Foundation of China (NSFC) under Grant 61001100, 61077009.

References

[1] `Z. Rahman, D. J. Jobson and G. A. Woodell, "Multiscale Retinex for color rendition and dynamic range compression", in Proc. SPIE 2847, **(1996)**, pp. 183.
[2] M. Y. Lee, C. H. Son, J. M. Kim, C. H. Lee and Y. H. Ha, "Illumination-Level Adaptive Color Reproduction Method with Lightness Adaptation and Flare Compensation for Mobile Display", Journal of Imaging Science and Technology, vol. 51, no. 1, **(2007)**, pp. 44-52.
[3] R. C. Gonzalez and R. E. Woods, "Digital Image Processing (second edition)", Pearson Education Asia Limited, **(2007)**.
[4] A. K. Jain, M. N. Murty and P. J. Flynn, "Data clustering: review", ACM Computer Surveys, vol. 31, ACM Press, **(1999)**, pp. 264-323.
[5] D. Ziou and S.Tabbone, "Edge detection techniques: an overview," International Journal of Pattern Recognition and Image Analysis, vol. 8, no. 4, **(1998)**, pp. 537-559.
[6] S. Chen and D. Zhang, "Robust image segmentation using FCM with spatial constraints based on new kernel-induced distance measure," IEEE Trans. Systems, Man and Cybernetics, Part B, vol. 34, no. 4, **(2004)** August, pp. 1907-1916.
[7] W. Wu, Z. Liu and X. He, "Learning-based super resolution using kernel partial least squares", Image Vision Comput., vol. 29, **(2011)**, pp. 394-406.
[8] W. Wu, Z. Liu, W. Gueaieb and X. He, "Single-image super-resolution based on markov random field and contourlet transform", J. Electron. Imaging, vol. 20, no. 023005, **(2011)**.
[9] W. Wu, Z. Liu and D. Krys, "Improving laser image resolution for pitting corrosion measurement using markov random field method", Autom. Constr., vol. 21, **(2012)**, pp. 172-183.
[10] W. Wu, Z. Liu, M. Chen, X. Yang and X. He, "An automated vision system for container-code recognition", Expert Systems with Applications, vol. 39, (2012), pp. 2842-285.
[11] W. Wu, X. Yang and X. He, "Handwritten numeral recognition by model reconstruction based on manifold learning", The 2007 International Conference on Information Computing and Automation (ICICA'07), **(2007)**.
[12] J. Wu, C. Liang, J. Han, Z. Hu, D. Huang, H. Hu, Y. Fang and L. Jiao, "A Two-Stage Lossless Compression Algorithm for Aurora Image Using Weighted Motion Compensation and Context-Based Model", Optics Communications, vol. 290, **(2012)**, October 22, pp. 19-27.
[13] Y. Fang, J. Wu and B. Huang, "2D sparse signal recovery via 2D orthogonal matching pursuit", Science China: Inf. Sci., vol. 55, **(2012)**, pp. 889-897.
[14] J. Wu, T. Li, T. -J. Hsieh, Y. -L. Chang and B. Huang, "Digital Signal Processor-based 3D Wavelet Error-resilient Lossless Compression of High-resolution Spectrometer Data", Journal of Applied Remote Sensing, vol. 5, no. 051504, **(2011)** November 28.
[15] A. Paul, J. Wu, J. -F. Yang and J. Jeong, "Gradient-based edge detection for motion estimation in H.264/AVC", IET Image Processing, vol. 5, no. 4, **(2011)**, pp. 323–327.
[16] J. Wu, J. Huang, G. Jeon, J. Jeong and L. C. Jiao, "An adaptive autoregressive de-interlacing method", Optical Engineering, vol. 5, no. 50, **(2011)**.
[17] J. Wu, A. Paul, Y. Xing, Y. Fang, J. Jeong, L. Jiao and G. Shi, "Morphological dilation image coding with context weights prediction", Signal Processing: Image Communication, vol. 25, no. 10, **(2010)**, pp. 717-728.
[18] M. Anisetti, C. A. Ardagna, E. Damiani, F. Frati, H. A. Müller and A. Pahlevan, "Web Service Assurance: The Notion and the Issues", Future Internet, vol. 4, no. 1, **(2012)**, pp. 92-109.
[19] M. Anisetti, C. A. Ardagna, V. Bellandi, E. Damiani, M. Döller, F. Stegmaier, T. Rabl, H. Kosch and L. Brunie, "Landmark-assisted location and tracking in outdoor mobile network", Multimedia Tools Appl., vol. 59, no. 1, **(2012)**, pp. 89-111.

[20] M. Anisetti, C. A. Ardagna, E. Damiani and J. Maggesi, "Security certification-aware service discovery and selection", SOCA, **(2012)**, pp. 1-8.
[21] M. Anisetti, C. A. Ardagna and E. Damiani, "A Low-Cost Security Certification Scheme for Evolving Services", ICWS, **(2012)**, pp. 122-129.
[22] M. Anisetti, C. A. Ardagna, V. Bellandi, E. Damiani and S. Reale, "Map-Based Location and Tracking in Multipath Outdoor Mobile Networks", IEEE Transactions on Wireless Communications, vol. 10, no. 3, **(2011)**, pp. 814-824.
[23] M. Anisetti, C. A. Ardagna, V. Bellandi, E. Damiani and S. Reale, "Advanced Localization of Mobile Terminal in Cellular Network", IJCNS, vol. 1, no. 1, **(2008)**, pp. 95-103.
[24] http://www.gipsa-lab.grenoble-inp.fr/~laurent.condat/imagebase.html.

Authors

Gwanggil Jeon received the BS, MS, and PhD (summa cum laude) degrees in Department of Electronics and Computer Engineering from Hanyang University, Seoul, Korea, in 2003, 2005, and 2008, respectively.

From 2008 to 2009, he was with the Department of Electronics and Computer Engineering, Hanyang University, from 2009 to 2011, he was with the School of Information Technology and Engineering (SITE), University of Ottawa, as a postdoctoral fellow, and from 2011 to 2012, he was with the Graduate School of Science & Technology, Niigata University, as an assistant professor. He is currently an assistant professor with the Department of Embedded Systems Engineering, Incheon National University, Incheon, Korea. His research interests fall under the umbrella of image processing, particularly image compression, motion estimation, demosaicking, and image enhancement as well as computational intelligence such as fuzzy and rough sets theories.

He was the recipient of the IEEE Chester Sall Award in 2007 and the 2008 ETRI Journal Paper Award.

